Journal of Radioanalytical and Nuclear Chemistry (2019) 322:763–769
https://doi.org/10.1007/s10967-019-06694-4

Analysis of anomaly characteristics of the soil gas radon from the crossing fault in the mid-east area of Qilian mountain before the 2016 Menyuan Ms6.4 earthquake

Chen-hua Li[1,2,3] · Hui Zhang[1,2] · He-jun Su[1,2] · Hui-ling Zhou[1,2]

Received: 11 June 2019 / Published online: 8 August 2019

Abstract
Based on the mobile monitoring network of tectonic geochemical in the Mid-East section of Qilian mountain, the precursory anomaly analysis and seismic situation tracking in the seismic hazard area were carried out by monitoring the concentration of soil gas radon crossing fault and combining with the distribution characteristics of seismic activity *b* value. Results show that the concentration of radon released changed significantly difference in the Mid-East segment of Qilian mountain during 2007–2013, under the background of the regional stress field enhancement, the gas release concentration of Gulang fault significantly decline, implying there is an obvious squeezing and the fault stress accumulation resulting in the decrease of porosity and radon concentration, so we circle a potential over magnitude 6 earthquake hazard fault segment in the future. Subsequently the 2016 Menyuan Ms6.4 earthquake occurred in this hazard zone. Therefore, we believe that soil gas radon can be used as a tracer for regional fault tectonic activities and stress changes, and it is necessary to pay attention to the monitoring of cross-fault soil gas in earthquake precursor observation.

Keywords Soil gas crossing fault · Menyuan Ms6.4 earthquake · Mid-East segment of Qilian · Hazard area

Introduction

On January 21, 2016, an Ms6.4 earthquake occurred in Menyuan County, Haibei Prefecture, Qinghai Province. The epicenter was at 37.68°N, 101.62°E, and the focal depth was 10 km. This earthquake was another strong earthquake that occurred in the Gansu-Qingdao border area after the Yushu 7.0 earthquake in 2012. The epicenter was located on the north side of the Lenglongling fault in Qilian–Haiyuan fault zone, belonging to the key monitoring area of the Mid-East section of the Qilian mountains [1, 2]. The Qilian–Haiyuan fault zone is an important active fault zone on the northeastern margin of the Qinghai–Tibet Plateau [3, 4], which is dominated by left-lateral strike-slip, and can be divided into the Tolashan fault, the Lenglongling fault, and the Jinqianghe fault, Maomaoshan fault, Laohushan fault and Haiyuan fault from west to east [5], and the east–west extension Gulang fault is separated eastward at 102.2°E [6–8].

In September 2007, through the "10th Five-Year Plan" and "National Earthquake Network Project", a tectonic geochemical flow monitoring network composing of 15 fault gas flow observation points was constructed in the Laohushan–Maomaoshan fault, Haiyuan fault and Gulang fault, and the survey of the observation points, the investigation of the tectonic geological background, the measurement of the background value of the fault gas and the construction of the protective signs of the points were completed. In September 2013, there were many anomalies in the fixed-point precursors and seismic activities of the Qilian mountains. Therefore, Gansu Earthquake Bureau initiated the short-term tracking of fault soil gas flow monitoring in this area. 10 mobile stations with stable background, determined structural position, and abnormal peaks in the fault observation network were selected to conduct cross-fault soil gas measurements (Fig. 1). The purpose of this short-term follow-up monitoring is to analyze the changes of soil gas

✉ Hui Zhang
zhanghuigsdzj@126.com

1 Earthquake Administration of Gansu Province, Lanzhou 730000, China

2 Lanzhou Institute of Seismology, CEA, Lanzhou 730000, China

3 Institute of Geochemistry, Chinese Academy of Sciences, Guiyang 550081, China

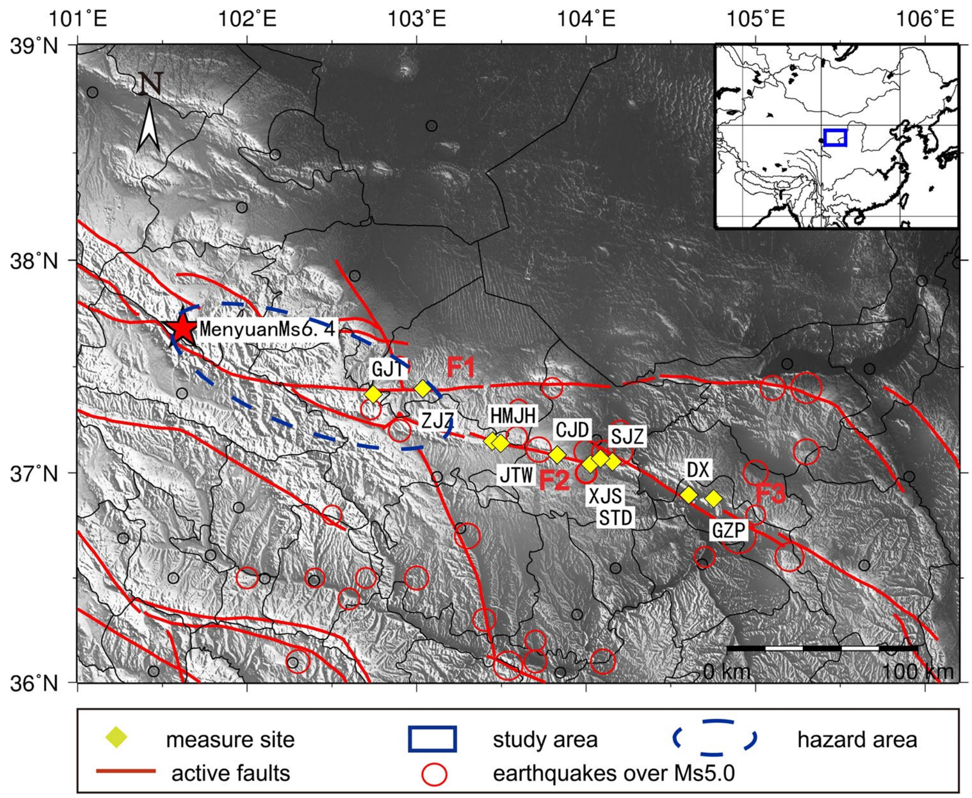

Fig. 1 Distribution of survey line and historical moderate and strong earthquakes (F1: Gulang fault; F2: Laohushan–Maomaoshan fault; F3: Haiyuan fault)

concentration through high-density fault soil gas distribution and measurement at Haiyuan fault, Laohushan fault and Gulang fault site, and to provide evidence of deep underground fluid activity for the faults and active sections that are at risk for earthquakes in the future and the location of future earthquakes. Through two comparative studies of flow monitoring, it was found that the Gulang fault had a significant decrease in soil gas concentration. The study believed that this section has obvious "shutting" characteristics and is a dangerous section with strong earthquakes of magnitude 6 in the future. On this basis, an elliptical danger zone with a short axis of 30 km and a semi-major axis of about 50 km was delineated, and the earthquake occurred in this area. Therefore, it provides a new idea for us to use the method of tectonic geochemistry to carry out scientific exploration of earthquake prediction.

Survey line distribution and instrument

Survey line layout

Your topic may require different sections (e.g. methods describing calculations or simulations). A *Review paper* certainly needs other sections: Abstract, Introduction, the reviewed topics one by one, and a conclusion. In the case of a review paper, it is even more important to give references to the latest papers appearing in the major journals of the field. A total of 10 fault soil radon gas survey lines were laid, and each survey line was set up with a measuring point every 10 m, a total of 117 measuring points. In order to avoid the influence of meteorological conditions, the field measurement work is carried out during the period when the meteorological conditions are relatively stable, and each measuring point is repeatedly measured. During the measurement process, the instrument is normal and has no other interference factors to ensure the stability and reliability of the measuring data. The survey lines are mainly concentrated on the western section of Gulang Fault, Laohushan–Maomaoshan Fault and Haiyuan Fault. Among them, the survey lines of Guanjiatai and Zhoujiazhuang are located in Gulang Fault, the survey lines of Heimaquanhe, Jintangwa, Cuijiadun and Xijishui survey lines are located in Laohushan–Maomaoshan Fault, whereas Santangdong, Shenjiazhuang, Daxian, Gaozaoping survey lines are located in Haiyuan Fault. The specific line layout is shown in Fig. 1 and Table 1.

Measuring instruments

The radon gas measurement was performed by SAPHYMO's AlphaGUARD P2000 portable tester with a standard deviation of < 3%. When sampling, first drill a 80 cm deep hole 80 cm with drilling steel, insert the sampler, and pump the soil gas to the instrument with a pump set at a flow rate of

Table 1 Site condition of survey line

Survey line code	Survey line name	Longitude (°)	Latitude (°)	Number of points/piece	Fault zone
GJT	Guanjiatai	102.74	37.37	10	Gulang fault
ZJZ	Zhoujiazhuang	103.04	37.40	26	
HMJH	Heimaquanhe	103.45	37.15	12	Laohushan–Maomaoshan fault
JTW	Jintangwa	103.50	37.14	21	
CJD	Cuijiadun	103.83	37.09	14	
XJS	Xijishui	104.03	37.04	13	
STD	Santangdong	104.08	37.07	10	Haiyuan fault
SJZ	Shenjiazhuang	104.16	37.05	11	
DX	Daxian	104.61	36.89	10	
GZP	Gaozaoping	104.75	36.88	11	

1 L/min. The sample volume is 1 L. The location of the profile line requires less vegetation, the vertical fracture is better, and the surface has the original cover with a certain thickness.

Measurement results

The soil gas concentration distribution of each site fault was analyzed separately, and the background value and abnormal upper and lower limits were calculated. The average concentration value of each line is taken as the background value K, and the lower limit of the fault gas anomaly is the background value + 2 mean square error ($K+2\delta1$) [9–12]. The shape of each line is shown in Fig. 2.

It can be seen from Fig. 2 that the soil radon gas concentration of the 10 fault gas sites measured by this short-term tracking is abnormal, and the peak curve characteristics are prominent. Most of the two measurements have abnormal points near the fault, which is very consistent. It can be seen that the measurement data of the cross-fault soil gas is stable and the measurement results are true and reliable. The results of the two-stage fault soil radon gas measurement are shown in Table 2.

Discussion

Characteristics of spatial distribution of fault gas concentration

Figure 3 is a spatial distribution map of the peak value of the cross-fault soil radon gas along the Gulang fault, the Laohushan–Maomaoshan fault and Haiyuan faults. It can be seen from the figure that the abnormal peak value of radon in Guanjiatai and Zhoujiazhuang sites on the Gulang fault in 2007 was 34.1986 Bq/L and 37.5846 Bq/L respectively. And the figures were 18 Bq/L and 10.2 Bq/L in 2013. The fault gas of both sites showed a significant decrease in release concentration.

The abnormal peak value of radon in Heimaquanhe, Jintangwa, Cuijiadun and Xijishui on the Laohushan–Maomaoshan fault was 11.17738 Bq/L, 4.2325 Bq/L and 9.3115 Bq/L and 6.9413 Bq/L respectively in 2007. The figures in 2013 were 13.7 Bq/L, 15.3 Bq/L, 9.25 Bq/L and 11.6 Bq/L respectively. The release concentration of fault gas increased, but without significant changes.

The abnormal peak value of radon in Santangdong, Shenjiazhuang, Daxian and Gaozaoping on the Haiyuan fault was 12.86668 Bq/L, 9.3115 Bq/L, 2.7088 Bq/L and 2.2009 Bq/L respectively in 2007. The figures in 2013 were 15.9 Bq/L, 14.6 Bq/L, 31.1 Bq/L and 17.4 Bq/L. It can be seen that the release concentration of fault gas was significantly improved. The most typical sites were Daxian and Gaozaozhuang, and the radon release concentrations increased by 11.48 and 7.9 times respectively.

Analysis of spatial distribution of fault gas concentration and seismic activity

Dynamic changes in b values are often employed to judge seismic activity, which is a coefficient in the famous Gutenberg–Richter formula (G–R). The G–R relationship, namely, the magnitude-frequency relationship, was first proposed by Gutenberg et al. [13]. The number of earthquakes $N(M)$ with a magnitude $\geq M$ within a certain period of time can be expressed by Eq. (1):

$$\log N(M) = a - bM \quad (1)$$

The parameter a represents the level of seismic activity in the area, and the parameter b describes the proportional relationship between large and small earthquakes [13]. The b value not only indicates the proportional relationship between big and small earthquakes, but is also closely related to the state of the geostress. Based on the inverse proportion between the geostress and the b value, Wiemer

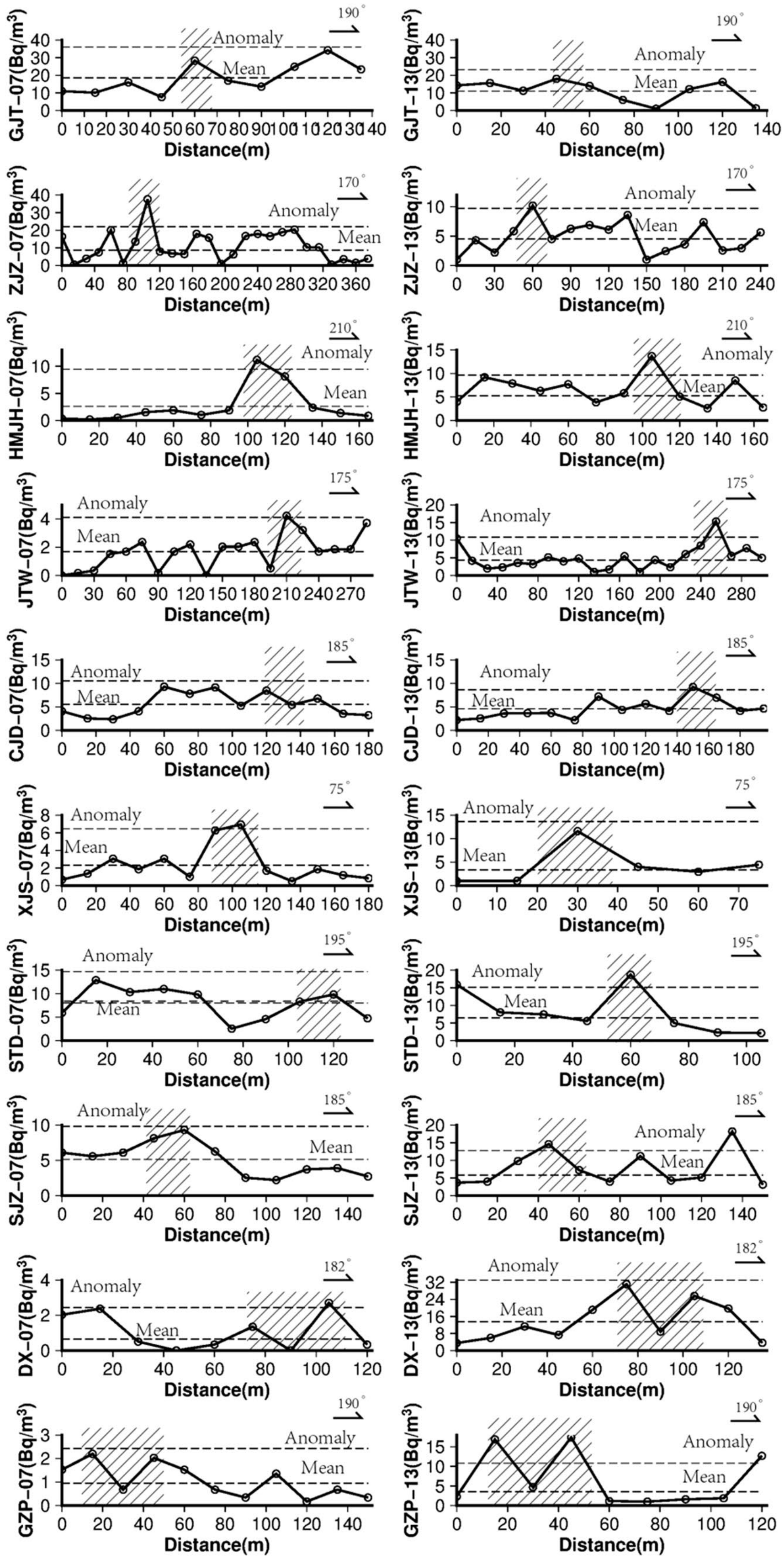

Fig. 2 The concentration curve of each line profile

Table 2 Measurement results of soil gas radon

Survey line code	Survey line length (m)	Direction finding	Rn/(Bq L^{-1})				Two-phase peak value ratio (13/07)
			2007		2013		
			Peak value	Background value	Peak value	Background value	
GJT	150	190°	34.1986	18.5891	18	10.942	0.53
ZJZ	390	170°	37.5846	10.9003	10.2	4.79	0.27
HMJH	180	210°	11.1738	2.5959	13.7	6.4442	1.23
JTW	315	175°	4.2325	1.6845	15.3	4.9318	3.61
CJD	210	185°	9.3115	5.5348	9.25	4.5879	0.99
XJS	195	75°	6.9413	2.3311	11.6	5.752	1.67
STD	150	195°	12.8668	7.991	15.9	6.46	1.24
SJZ	165	185°	9.3115	5.1406	14.6	5.8182	1.57
DX	150	182°	2.7088	1.0722	31.1	13.606	11.48
GZP	165	190°	2.2009	1.0466	17.4	6.6233	7.91

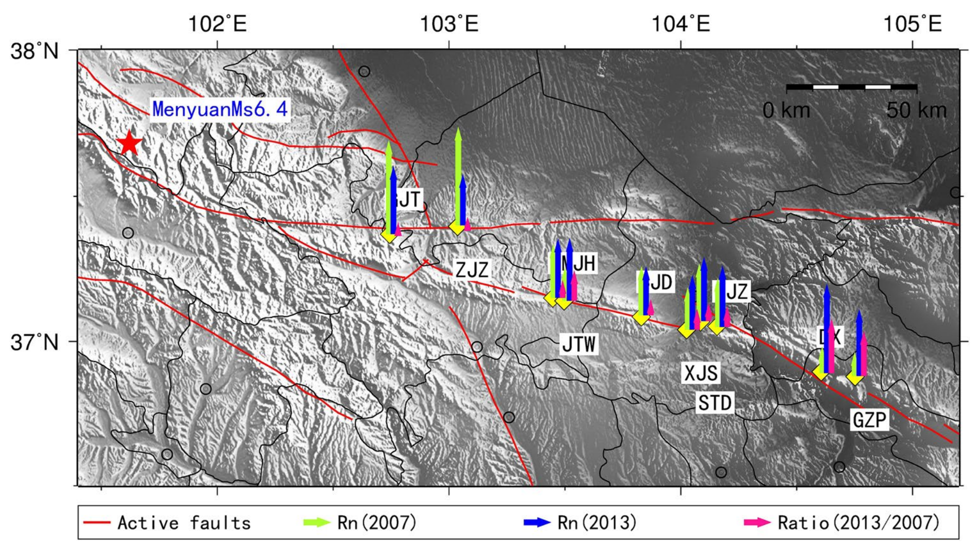

Fig. 3 Spatial distribution of ratio of abnormal peak value and maximum value of soil gas radon concentration in the Mid-East segment of Qilian mountains

et al. [14] and Wyss et al. [15] once used the spatial distribution of the *b* value to study the spatial distribution of the current relative geostress level of the active fault zone and distinguish the relatively high stress accumulation segment or concave-convex body segment. Yi et al. [16] used the spatial distribution of *b* value to determine the relative level of relative stress accumulation in different segments of the active fault zone, and thus judged the current activity habits and strong earthquake hazard segments of different sections in the fault zone. According to the study, the high *b* value indicates high frequency of small earthquake, small risk of middle-strong earthquake, and the relatively low regional stress accumulation level. On the contrary, the low *b* value shows low frequency of small earthquake, high risk of middle earthquakes, and high level of regional stress accumulation. In this paper, the ZMAP program and the 1980–2013 seismic data are used for spatially scanning and calculating the *b* value of the Mid-East segment of the Qilian mountains, where the maximum likelihood method is employed. The lower limit of the integrity magnitude M_{min} is 1.8 [17], the grid division is $0.1° \times 0.1°$ and the scanning radius is 50 km.

Figure 4 is a spatial distribution map of *b* value of seismic activity parameters in the Mid-East of Qilian mountains. It can be seen from the figure that the *b* value of seismic activity parameters in the Mid-East of Qilian mountains is generally characterized by high-east and low-west in space, and has obvious segmentation. The high *b* value is mainly concentrated in the Jingtai-Baiyin Dayingshui Basin in the Mid-East of the fault zone, while low *b* value is mainly concentrated in the west of the fault. This is consistent with the previous study of fault gas concentration, indicating a certain correlation between active fault gas concentration and seismic activity. Therefore, the author believes that the fault gas in the Mid-East segment of the Qilian mountains

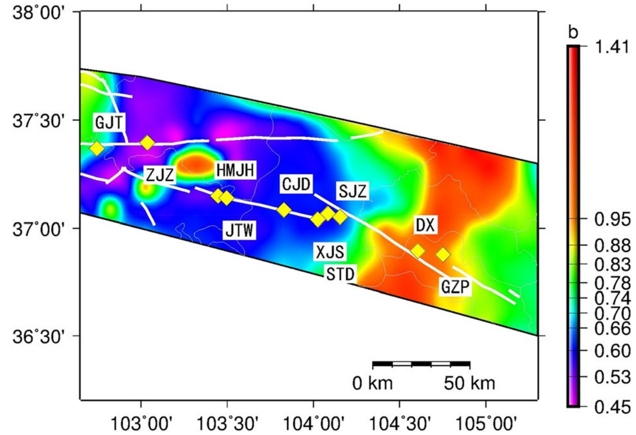

Fig. 4 The spatial distribution of *b* value in the Mid-East segment of Qilian mountains

can be used as a measurement tool for regional fault tectonic activity and stress change, and serves as an effective precursor observation method for long-term flow observation of earthquake workers.

Analysis of seismic hazard segments

The spatial distribution characteristics of the abnormal peak value of the radon gas concentration in the cross-fault soil show that the fault gas release rates of the Gulang, Laohushan–Maomaoshan and Haiyuan faults in the Mid-East of Qilian mountains changed significantly during 2007–2013. Among them, the concentration of fault gas released from the Haiyuan fault in which the historical earthquake occurred increased rapidly, indicating that the regional stress in the Mid-East of the Qilian mountains is further enhanced. Under the background of regional stress field enhancement, the gas release concentration in the northwestern part of the Gulang fault decreased significantly, which reflected the obvious extrusion and stress accumulation in the region, and thus resulted in a decrease in porosity and a decrease in the release concentration of radon. It is the fault section at the risk of the earthquake above Ms.6 (Fig. 5). On this basis, we make an elliptical danger zone with a short axis of 30 km and a semi-major axis of about 50 km in the northwestern part of the Gulang fault, and this Ms6.4 earthquake occurred in this area.

Conclusions

In summary, earthquake prediction is one of the present scientific problems. There have been successful experiences in earthquake prediction in China, and also many lessons of failure. The scientific thinking of earthquake prediction must be based on a certain physical mechanism. The author believes that according to the sensitivity and convenience of fault gas, the survey line can be directly placed on the dangerous fault for flow tracking, monitoring the development process of the "source" area, thereby avoiding the limitations of the spring and well exposure locations used by underground fluid means. The fact that a good forecasting opinion was proposed before the Qinghai Menyuan Ms6.4 earthquake indicates that fault soil gas can be used as a measure of regional fault tectonic activity and stress change, and can also be used as an effective precursor observation method for long-term flow observation.

Therefore, our general idea is to hierarchically track the location of the earthquake site from the "earthquake empty space" at the large spatial–temporal scale to the "precursor space in the epicenter" of the small area, and to the "blocking section" of the active fault, that is, the "weak fluid active section". In addition, the magnitude of the potential seismic hazard segment based on the degree of activity of the regional seismic activity fault and the spatial scale of the locked segment is determined. Through monitoring the

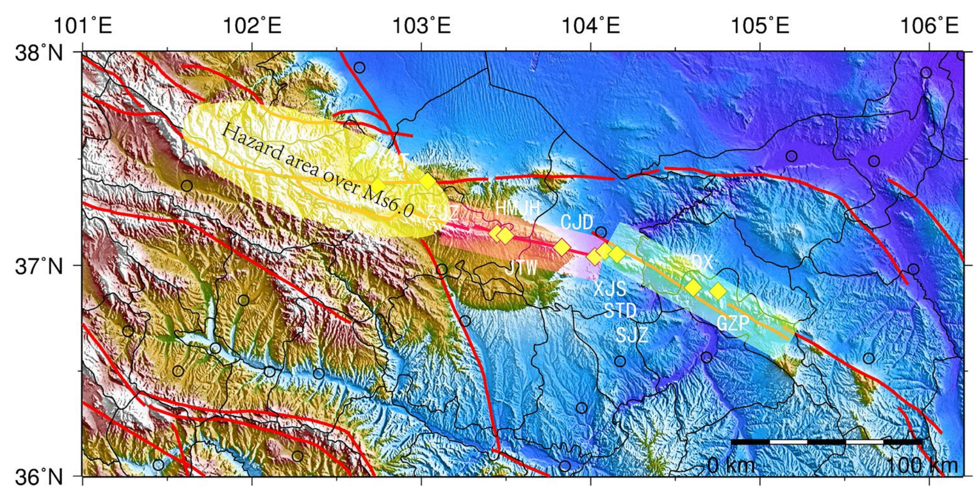

Fig. 5 Seismic risk analysis of geochemical methods in the Mid-East segment of Qilian mountains

characteristics of the abnormal changes in the internal and both ends of the weak fluid active section over time, we will strive to capture the short-term and short impending information.

Acknowledgements This work is supported by the basic R&D fund of the Institute of Earthquake Science, China Earthquake Administration (CEA) (Grant 2018IESLZ05), the Gansu province science and technology plan project (Grant 1606RJYA218) and Spark Program of China Earthquake Administration (Grant XH15043). The authors wish to thank the Editor and two reviewers for their fruitful comments on an earlier version of the manuscript.

References

1. Dongning L, Jie L, Shumei L et al (2018) Discussion on the seismogenic structure of the 2016 Menyuan Ms6.4 earthquake in Menyuan, Qinghai. Seismol Geol 40(1):107–120
2. Fang L, Yiqing Z, Yunfeng Z (2019) Frequency characteristics of continuous gravity before the 2016 Menyuan MS6.4 earthquake. China Earthq Eng J 41(2):469–475
3. Peltzer G, Tapponnier P (1988) Formation and evolution of strike-slip faults, rifts, and basins during the India-Asia Collision: an experimental approach. J Geophys Res 93:15085–15117
4. Tapponnier P, Molnar P (1977) Active faulting and tectonics in China. J Geophys Res 82:2905–2930
5. Zheng WJ, Zhang PZ, He WG, Yuan DY, Shao YX, Zheng DW, Ge WP, Min W (2013) Transformation of displacement between strike-slip and crustal shortening in the northern margin of the Tibetan Plateau: evidence from decadal GPS measurements and late Quaternary slip rates on faults. Tectonophysics 584:267–280
6. Wen-gui H, Dao-yang Y, Wei-peng G et al (2010) Determination of the slip rate of the Lenglongling fault in the middle and eastern segments of the Qilian Mountain active fault zone. Earthquake 30(1):131–137
7. Peng G, Zhu-jun H, Yan-fen A et al (2017) Activity of the Lenglongling fault system and seismotectonics of the 2016 MS6.4 Menyuan earthquake. Sci China (Ser D) 60(5):929–942
8. Zengjian G, Anning G, Xianghong Z et al (2017) Commemoration of the ninetieth anniversary of the Gulang M_S8 earthquake—discussion of the study of great earthquakes. China Earthq Eng J 39(2):191–195
9. Hejun S, Hui Z, Chenhua L et al (2013) Geochemical features of fault gas on northern margin fault of Xiqinling and its seismic hazard analysis. China Earthq Eng J 35(3):671–676
10. Li Chenhua S, Hejun ZH et al (2016) Correlation between the spatial distribution of radon anomalies and fault activity in the northern margin of West Qinling Fault Zone, Central China. J Radioanal Nucl Chem 308:679–686
11. Zhou Huiling S, Hejun ZH et al (2018) Mobile monitoring network layout technique for fault gas based on seismogenic mode. China Earthq Eng J 40(5):1052–1060
12. Yang Z, Bo D, Han S et al (2017) Study on the geochemical characteristics of radon in the Jiangsu section of the Tanlu fault zone. China Earthq Eng J 39(2):248–252
13. Gutenberg B, Richter CF (1944) Frequency of earthquakes in California. Bull Seismol Soc Am 34(4):185–188
14. Wiemer S, Wyss M (1997) Mapping the frequency-magnitude distribution in asperities: an improved technique to calculate recurrence times? J Geophys Res 102(B7):15115–15128
15. Wyss M, Schorlemmer D, Wiemer S (2000) Mapping asperities by minima of local recurrence time: San Jacinto-Elsinore fault zones. J Geophys Res 105(B4):7829–7844
16. Guixi Y, Xueze W (2007) The application and limitation of multiple seismicity parameters to assessing current faulting behavior and seismic potential of active fault zones. Seismol Geol 29(2):254–271
17. Jiangang F, Changsheng J, Libo H et al (2012) Analysis on the monitoring capability of seismic networks and completeness of earthquake catalogues in Gansu region. Acta Seismol Sin 34(5):646–658